

Figure 2. Structure of the fire parameterization of pyrE. Processes related to atmospheric properties are in blue, surface properties are in green, ignition and suppression are in yellow and gray, and fire properties are in red.

initial analysis showed that with the original Pechony and Shindell (2009) suppression scheme fire activity is overestimated in the TENA and Middle East (MIDE) regions, while being underestimated in NHAF and SHAF. Following these initial results, a series of sensitivity simulations were conducted with varying values of suppression coefficients. The final values were chosen in a heuristic manner that improved the simulations yet did not over-fit them to the observations, similarly to Pechony and Shindell (2009) and other fire parameterization, due to the lack of appropriate global data.

We use the complement of the fraction of suppressed fires that is the fraction of non-suppressed fires, f_{NS} :

$$f_{NS} = \begin{cases} 0.2\exp(-0.05PD), & \text{USA and MIDE;} \\ 1, & \text{Africa;} \\ 0.05 + 0.9\exp(-0.05PD), & \text{elsewhere.} \end{cases} \quad (6)$$

2.4 Active fires

Active fires are a key metric used to drive burned area and fire emissions in pyrE. The number of fires in a time step per square kilometer is calculated as the product of flammability, sum of natural and anthropogenic ignition, and suppression (Pechony and Shindell, 2009) (Fig. 2):

$$N_{\text{fire}}(t)_{i,j} = F(t)_{i,j} \cdot (I_N(t)_{i,j} + I_A(t)_{i,j}) \cdot f_{NS}(t)_{i,j}. \quad (7)$$

2.5 Burned area (BA)

We adopted the process-based approach by Li et al. (2012) to calculate fire spread and burned area. The burned area in grid cell (i, j) at a model time step t is the product of active fires and the weighted average over plant functional types (PFTs) of the area burned by one fire:

$$BA_{i,j} = N_{\text{fire}}(t)_{i,j} \cdot \sum_v a_{i,j,v} \cdot f_{i,j,v}, \quad (8)$$

where $f_{i,j,v}$ is the fractional area covered by plant functional type v , and the burned area of a single fire $a_{i,j,v}$ is assumed to have an elliptical shape (Fig. 3). Wind speed, surface relative humidity, and vegetation type control the eccentricity of the

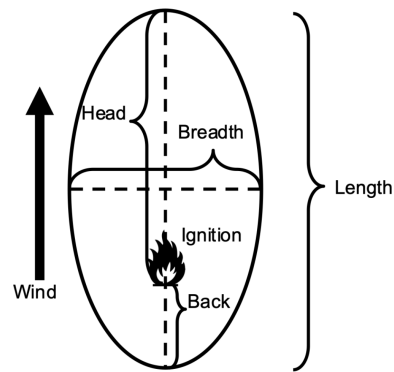


Figure 3. Approximation of a single fire spread. Based on van Wagner (1969) and Arora and Boer (2005).

ellipsoid that represents the burned area of a single fire (based on van Wagner, 1969):

$$a_{i,j,v} = \frac{\pi \text{ROS}^2 \tau^3}{4\text{LB}} \left(1 + \frac{1}{\text{HB}}\right)^2, \quad (9)$$

where ROS is the rate of fire spread, LB is the length-to-breadth ratio, and HB is the head-to-back ratio. The stronger the wind, the more eccentric the ellipse, i.e., the bigger the length-to-breadth ratio:

$$\text{LB} = 1 + 10 \cdot (1 - \exp(-0.06W)), \quad (10)$$

where W is the surface wind speed (in m s^{-1}).

Strong winds also increase the head-to-back ratio CE1 CE2, the ratio of the downwind spread compared to the upwind spread:

$$\text{HB} = \frac{\text{LB} + \sqrt{\text{LB}^2 - 1}}{\text{LB} - \sqrt{\text{LB}^2 - 1}}. \quad (11)$$

The rate of spread (ROS) of a fire is a function of vegetation type, wind speed, and atmospheric and soil moisture:

$$\text{ROS} = \text{ROS}_{\text{max}} \cdot gW \cdot f_{RH} \cdot f_{\theta}. \quad (12)$$